agriculture

MDPI

Article

Study on Path Planning in Cotton Fields Based on Prior Navigation Information

Meng Wang [1,2], Changhe Niu [3], Zifan Wang [1], Yongxin Jiang [3], Jianming Jian [1] and Xiuying Tang [1,*]

[1] College of Engineering, China Agricultural University, Beijing 100083, China; wm15@xjie.edu.cn (M.W.); s20213071234@cau.edu.cn (Z.W.); jamesjian@cau.edu.cn (J.J.)
[2] School of Mechanical and Electrical Engineering, Xinjiang Institute of Engineering, Urumqi 830023, China
[3] Research Institute of Agricultural Mechanization, Xinjiang Academy of Agricultural Sciences, Urumqi 830091, China; xjnch@xaas.ac.cn (C.N.); jyx@xaas.ac.cn (Y.J.)
* Correspondence: txying@cau.edu.cn; Tel.: +86-159-1060-4652

Abstract: Aiming at the operation scenario of existing crop coverage and the need for precise row alignment, the sowing prior navigation information of cotton fields in Xinjiang was used as the basis for the study of path planning for subsequent operations to improve the planning quality and operation accuracy. Firstly, the characteristics of typical turnaround methods were analyzed, the turnaround strategy for dividing planning units was proposed, and the horizontal and vertical operation connection methods were put forward. Secondly, the obstacle avoidance strategies were determined according to the traits of obstacles. The circular arc–linear and cubic spline curve obstacle avoidance path generation methods were proposed. Considering the dual attributes of walking and the operation of agricultural machinery, four kinds of operation semantic points were embedded into the path. Finally, path generation software was designed. The simulation and field test results indicated that the operation coverage ratio $C_R \geq 98.21\%$ positively correlated with the plot area and the operation distance ratio $D_R \geq 86.89\%$ when non-essential reversing and obstacles were ignored. C_R and D_R were negatively correlated with the number of obstacles when considering obstacles. When considering non-essential reversing, the full coverage of operating rows could be achieved, but D_R would be reduced correspondingly.

Keywords: agricultural machinery path planning; sowing navigation information; turnaround; obstacle avoidance; prior semantic map

Citation: Wang, M.; Niu, C.; Wang, Z.; Jiang, Y.; Jian, J.; Tang, X. Study on Path Planning in Cotton Fields Based on Prior Navigation Information. *Agriculture* **2024**, *14*, 2067. https://doi.org/10.3390/agriculture14112067

Academic Editor: António Luís Gomes Valente

Received: 3 September 2024
Revised: 15 October 2024
Accepted: 14 November 2024
Published: 16 November 2024

1. Introduction

China is the world's largest cotton producer, and Xinjiang is the largest cotton production area in China [1]. In 2023, the cotton planting area in China was 2788.1 thousand hectares, and Xinjiang accounted for approximately 85.3% [2]. Xinjiang cotton fields are relatively flat, with large plot sizes and fewer fixed obstacles, which are favorable for auto-driving operations using satellite navigation.

Path planning is a prerequisite for conducting auto-driving operations by agricultural machinery. Currently, the primary satellite navigation-assisted driving system mainly adopts the A-B line [3] for the path planning of agricultural machinery in large fields, and this is simple to operate and, supplemented by manual turnaround, obstacle avoidance, and process supervision, can satisfy most basic operations. It is also the main path planning method for cotton sowing in Xinjiang. Many studies have been conducted on turnaround methods (U-turn, bow-turn, Ω-turn, fishtail-turn, etc.) [4,5], routing planning (open-row, closed-row, shuttle, nesting, detouring, etc.) [6,7], and obstacle handling [8,9] to realize fully automated driving operations. Other methods have also been proposed based on conventional methods. Cariou [10] and Boryga [11] et al. presented a turnaround method based on cyclotron and polynomial curves, respectively. Zhang et al. introduced a fishtail-turn method with Two-back and Three-cut [12]. Boryga et al. raised a turnaround method

based on transition curves [13]. Hu et al. designed a Bessel curve obstacle avoidance path for circular obstacles [14]. Zhao et al. sought a point-to-point collision-free path for the tractor based on the minimum capture algorithm [15]. Xu et al. considered kinematic constraints and performed obstacle avoidance path planning based on the particle swarm algorithm [16]. Research was also carried out on this basis for full coverage path planning. Wu et al. proposed a full-coverage path planning method for agricultural robots based on an improved genetic algorithm [17]. Höffmann et al. presented an optimal coverage path planning for agricultural vehicles with curvature constraints by combining the modular approach and generalized traveling salesman problem [18]. Wu et al. put forward a smooth path planning algorithm based on Hybrid A* and Reeds-Shepp curves [19]. Šelek et al. introduced a gyratory curve-based method for the generation of smooth full-coverage paths [20]. Additionally, some scholars have realized path planning for irregular plots by region splitting, subregion traversal, and subregion connection [21–23]. Zhai et al. utilized block nesting to improve the adaptability of quadrilateral plots [24].

However, the above research was more applicable to work scenarios without crop cover (e.g., tillage, sowing, etc.) or without row-to-row requirements (e.g., lawn mowing), etc. There has been relatively less research on how to better utilize navigation data during sowing for more practical path planning in scenarios where there is already crop coverage and precise alignment is required, such as in cotton harvesting and straw and residue film recycling. Meanwhile, Xinjiang has actively promoted the use of precision planters equipped with Beidou satellite navigation in recent years, and this is already in full-scale use as of 2024 [25], accumulating a significant amount of path data. Applying the sowing navigation data as the target path for cotton harvesting and residual film recycling is more in line with the operational reality than the idealized path planning, and more conducive to enhancing the efficiency and accuracy of path planning, reducing the cost, and, more importantly, improving the corresponding operational accuracy.

According to the operational characteristics of Xinjiang cotton mulching sowing (mulching, laying drip irrigation tape, sowing, and covering soil all at once) [25], the precision planters equipped with Beidou satellite navigation can achieve automatic driving during straight operations, but manual driving is required for turning and obstacle avoidance. Therefore, the navigation path data during sowing have the following features: (1) The turnaround path cannot be used directly. In manual turnaround without considering the subsequent path data cycle reuse, the standardization of the path is insufficient, and there is redundancy and a mess, which may contain multiple reversals and repeated paths. It is not suitable for autonomous driving operations and has poor tolerance for vehicle turning radius. (2) The operation routing is not standardized, and human factors have a significant impact. There is less consideration for operational costs and greater randomness due to manual turnaround. Additionally, the original operational sequence may not apply to other agricultural machinery owing to the presence of different turning radii. (3) Obstacle avoidance paths cannot be used directly. The manual takeover of the agricultural machine is typically required for obstacle detour, and the detour path has strong personal habits, making it unsuitable for direct use in autonomous driving. (4) There is a lack of reasonable connections between horizontal and vertical working areas, usually achieved by manual driving. Additionally, the stored data are generally in the geodetic coordinate system, which needs to be converted to a planar cartesian coordinate system to facilitate the subsequent path tracking control.

Thus, this paper employs the operation coverage rate and operation distance ratio as evaluation indicators based on the sowing navigation data in Xinjiang cotton fields and describes path planning research on the basis of the sowing navigation data processing. Its aims are to (1) analyze the turnaround methods, specify the turnaround strategy, generate turnaround and horizontal–vertical connection paths, and then determine the operation routing; (2) clarify the obstacle avoidance strategy, determine the obstacle avoidance path generation method, and embed the operational semantic instructions; and (3) design the path generation software and conduct experimental analysis to obtain prior semantic maps

for cotton harvesting, residual film recycling, etc., and provide target paths for subsequent auto-driving operations of the corresponding agricultural machines to achieve higher work quality and efficiency.

2. Materials and Methods

2.1. Overall Design

2.1.1. Raw Information Analysis

Take the sowing navigation data of a cotton mulching planter in a place in Bazhou, Xinjiang, on 18 April 2024, as an example, as shown in Figure 1, with an operating area of 45.49 acres. The green path in the figure indicates auto-driving operation, the blue path indicates artificial driving, and the missing places of the data (e.g., at a in Figure 1) are the obstacle parts that need to be detoured manually. The regular blue line segment in the green line (e.g., at b in Figure 1) is generally a brief manual takeover of driving to sort out farm supplies and can be equated with the green path in subsequent operations without detouring. To facilitate vehicle turnarounds while improving land utilization, cotton sowing involves not only vertical operations along the long side but also horizontal operations perpendicular to the long side, commonly known as "pulling horizontal heads". Horizontal sowing is generally performed after the vertical operations are completed.

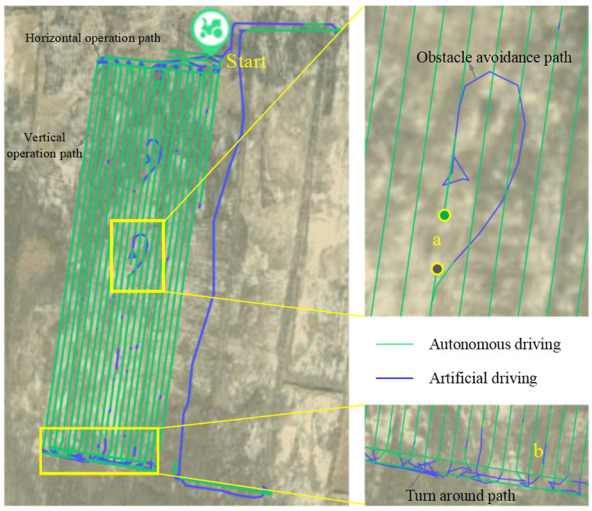

Figure 1. Example of navigation paths for cotton mulching sowing.

Xinjiang cotton mulching planting (with a standard film width of 2.05 m, generally) often adopts wide–narrow rows [26], as shown in Figure 2. The sowing width is often larger than the residual film recycling width, so it is necessary to translate the navigation line. The sowing width is 4.56 m, with two films per machine, and the residual film recycling width is 2.20 m with one film per machine. Therefore, the sowing navigation line needs to be shifted left and right by 1.14 m to obtain the navigation line for the residual film recycling.

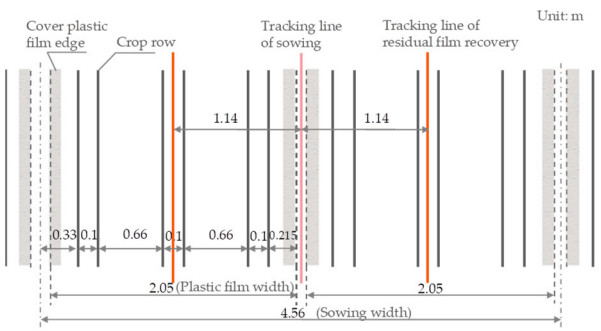

Figure 2. Schematic diagram of wide–narrow row cotton planting.

2.1.2. Design Processes

The overall design process of path planning is shown in Figure 3a. Path planning is carried out according to the prior information such as sowing navigation information, planting agronomy, and vehicle parameters, combined with path generation algorithms such as turnaround, obstacle avoidance, etc. The schematic representation of the planning results is shown in Figure 3b. The planning process is as follows.

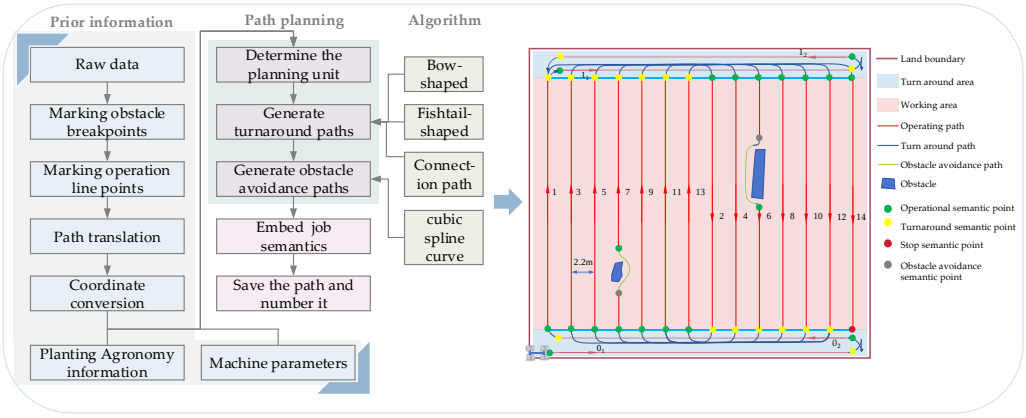

(**a**) (**b**)

Figure 3. The overall design process of prior semantic map. (**a**) Planning process; (**b**) schematic of planning results.

Firstly, the sowing navigation data are processed. This mainly involves marking the breakpoint coordinates of the missing parts and filling them in new columns of the table to estimate the range of obstacles for generating obstacle avoidance paths; excluding the manually driving portion based on sign position and labeling the coordinates of the horizontal and vertical operation endpoints; translating coordinates based on planting agronomy and filling in new columns of the table for generating the turnaround and connection paths; and converting WGS84 (World Geodetic System 1984) coordinates to UTM (Universal Transverse Mercator) coordinates.

Secondly, based on the above processed data, the full-coverage operation path is generated by combining the path generation methods of turnaround, obstacle avoidance, and horizontal–vertical operation connection under the constraints of vehicle parameters and planting agronomy.

Finally, the endpoint coordinates are labeled as function points and embedded with semantics to facilitate the coordination of actions between operations and walking and the map is numbered and imported into the map library for subsequent use of path tracking control.

2.2. Turnaround Path and Operation Routing

2.2.1. Turnaround Methods

Turnaround can be regarded as an optimization problem under multiple constraints such as vehicle turning radius, operation width, starting and ending postures, size of the turnaround area, operation direction and starting orientation, etc. The optimization objective is to connect all the operation rows with the appropriate turnaround width and the shortest total turnaround distance, i.e., to generate the optimal turnaround path with the smallest cost. Since time, energy consumption, and distance are the main costs of turnaround and they are positively correlated, the distance cost can be approximated as the total cost.

The U-turn, bow-turn, fishtail-turn, and Ω-turn methods commonly used by agricultural machinery are shown in Figure 4. The relationship between the minimum turning radius R and the operating width W determines the turnaround method. When $R \leq W/2$,

U-turn method has the least cost and is without reverse. When R > W/2, either Ω-turn or fishtail-turn methods can be selected, and the two can be substituted for each other. Fishtail-turn method has a lower energy cost than Ω-turn method but requires higher turning performance when reversing. Ω-turn method needs no reverse, but the required turning area is larger than that of the fishtail-turn method, especially when the turning radius is larger. When R > W/2, the bow-turn method, a deformed version of the U-turn method, can also be used to achieve turnaround through cross-row operations without the need for reversing and with a smaller turnaround width but with repeated paths. Considering that both the cotton harvester and the residual film recycling machine are large and not easy to turn around, the bow-turn method is prioritized in this paper, which has also been verified according to the literature as less costly [22], and the long side is usually used as the starting direction [5].

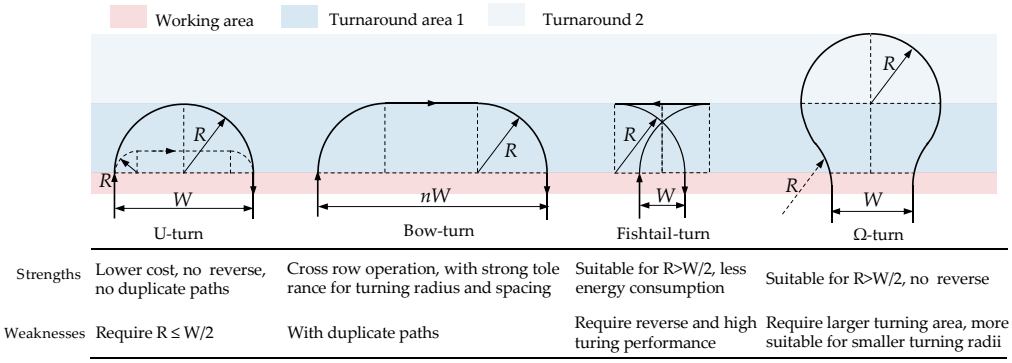

Figure 4. Commonly used turnaround paths for agricultural machinery.

Dubins curve, which is the shortest path connecting two two-dimensional planes under the condition that it satisfies curvature constraints and tangent directions at the start and end points, and assumes that the vehicle can only travel forward, was proved by Lester Eli Dubins in 1957, and the same result was later proved by Pontryagin's maximum principle [27]. Dubins curve consists of circular arcs with maximum curvature and straight lines, and the shortest path planning from one attitude to another can be realized by the suitable combination, which can effectively plan the path, reduce the energy consumption, and improve the efficiency. The set of paths {LSL, RSR, RSL, LSR, RLR, LRL} is given [28], where L and R denote the circular motions to the left and right, respectively, and S denotes the linear motion. The core idea of the Dubins curve is consistent with the need for agricultural machinery to turn around. Taking the RSR (line A'B' in Figure 5) path as an example, the bow-turn is a special form of the RSR path (line AB in Figure 5), i.e., the tangent line at the endpoint coincides with the operation row, and the consecutive turnaround can be regarded as the combination of RSR and LSR. Therefore, the idea of the Dubins curve also verifies the superiority of bow-turn method. This paper uses the bow-turn method and utilizes the idea of the Dubins curve for turnaround path planning.

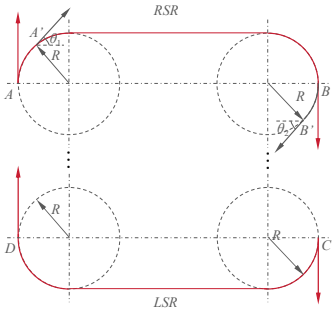

Figure 5. RSR and LSR paths of Dubins curves.

2.2.2. Turnaround Strategy

Unlike Dubins curves, agricultural machinery turnaround is simultaneously constrained by the operation width in addition to the minimum turning radius. When the bow-turn is used for a plot, it can be achieved in two ways as an overall operation or by dividing the planning unit.

(1) Overall operation: This takes the center row of the plot as the first crossing boundary, i.e., there is only one planning unit (refer to the schematic of the planning results in Figure 3). The cost function for the turnaround path is as follows:

$$\begin{cases} D_{total} = \frac{n_{total}}{2}\left(\frac{n_{total}}{2}W - 2R + \pi R\right) + \left(\frac{n_{total}}{2} - 1\right)\left[\left(\frac{n_{total}}{2} - 1\right)W - 2R + \pi R\right], n_{total} \in \text{even} \\ D_{total} = \left(\frac{n_{total}-1}{2} + 1\right)\left(\frac{n_{total}-1}{2}W - 2R + \pi R\right) + \frac{n_{total}-1}{2}\left[\left(\frac{n_{total}-1}{2} - 1\right)W - 2R + \pi R\right] + L_L, n_{total} \in \text{odd} \end{cases} \quad (1)$$

Here, D_{total} indicates the total distance of turnaround; n_{total} indicates the total number of operating rows; n_{unit} indicates the number of rows traversed by a planning unit; W indicates the operation width; R indicates the minimum turning radius of the vehicle; L_L indicates the length of a single operating row.

(2) Dividing the planning unit:

The overall operation rows are divided into several planning units, as shown in Figure 6a. When n_{uint} is odd, there will be repeated traversal of the center row or the end of the unit exit in the center row, as illustrated in Figure 6b. Therefore, n_{uint} is usually taken as an even number to reduce the number of duplicate paths and ensure that the planning units are connected at the beginning and end. n_{unit} with the smallest D_{total} is calculated as the optimal number of planning unit rows n; then, the cost function of the turnaround path is as follows:

$$\min_{n_{unit}}(D_{total}) \begin{cases} D_{total} = round\left(\frac{n_{total}-1}{n_{unit}-1}\right)\left\{\frac{n_{unit}}{2}\left(\frac{n_{unit}}{2}W - 2R + \pi R\right) + \left(\frac{n_{unit}}{2} - 1\right)\left[\left(\frac{n_{unit}}{2} - 1\right)W - 2R + \pi R\right)\right]\right\} \\ \left(\frac{n_{unit}}{2} - 1\right)W \geq 2R \\ n_{unit} \leq round\left(\frac{n_{total}}{2}\right), \ \& \ n_{unit} \in \text{even number} \end{cases} \quad (2)$$

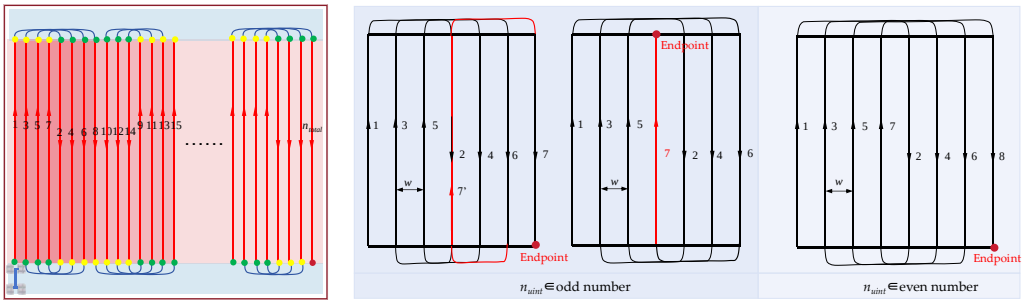

(**a**) (**b**)

Figure 6. Schematic diagram of dividing the planning unit with nesting operation. (**a**) Schematic diagram of dividing the planning unit; (**b**) examples of traversal effect when n_{uint} takes odd and even numbers.

Here, *round* denotes the downward rounding function.

When $(n_{total} - 1)/(n_{unit} - 1)$ is not divisible, the remaining operation rows adopt the fishtail-turn method considering the turnaround area constraints.

From the above turnaround function, it can be seen that the total distance traveled by the operation mode of dividing the planning unit is obviously smaller than the overall operation mode, and there are fewer repeated paths. Therefore, this paper gives priority to the dividing planning unit mode, and from Figure 6, it is clear that the operation route can be clarified while determining the turnaround path.

2.2.3. Bow-Turn Path Function

The schematic diagram of the bow-turn path is presented in Figure 7. Combining the standard equation of the circle with the piece-wise function, the single bow-turn path function is expressed in Equation (3) when working clockwise for example.

$$\begin{cases} y = \pm\sqrt{R^2 - (x - x_2)^2} + y_1, & \text{if } i \in \text{odd}, x_1 \le x < x_2 \\ & \text{if } i \in \text{even}, x_2 \le x < x_1 \\ y = y_2, x_2 \le x \le x_3, & \text{if } i \in \text{odd}, x_2 \le x < x_3 \\ & \text{if } i \in \text{even}, x_3 \le x < x_2 \\ y = \pm\sqrt{R^2 - (x - x_3)^2} + y_1, & \text{if } i \in \text{odd}, x_3 \le x < x_4 \\ & \text{if } i \in \text{even}, x_4 \le x < x_3 \end{cases} \quad (3)$$

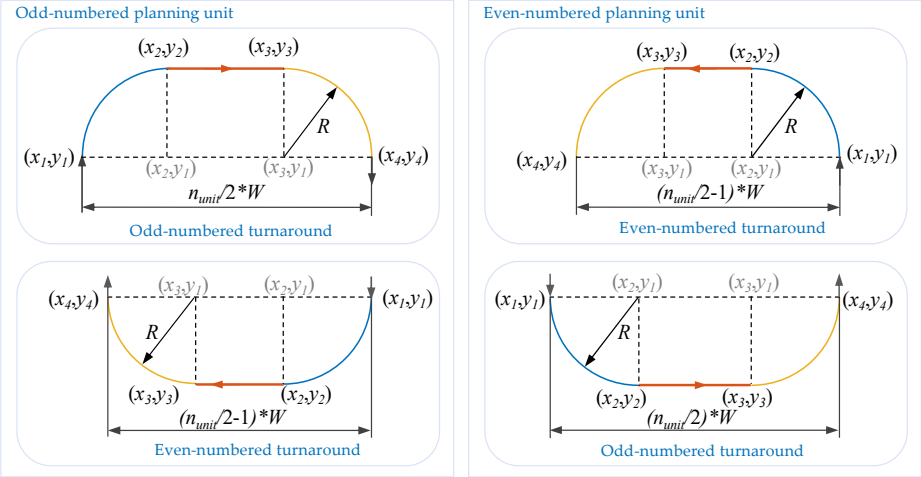

Figure 7. Schematic diagram of the bow-turn path.

Here, for the odd-numbered planning unit, Equation (3) takes a positive sign for odd-numbered turnarounds, and a negative sign for even-numbered turnarounds, and

$$\begin{cases} (x_2, y_2) = (x_1 \pm R, y_1 \pm R) \\ (x_3, y_3) = (x_1 \pm \partial w \mp R, y_1 + R) \\ (x_4, y_4) = (x_1 \pm \partial w, y_1) \end{cases}, \quad \begin{array}{l} \text{if } i \in \text{odd\&} \ j \in \text{odd}, \partial = \frac{n_{unit}}{2} \\ \text{if } i \in \text{odd\&} \ j \in \text{even}, \partial = \frac{n_{unit}}{2} - 1 \end{array}$$

For the even-numbered planning unit, Equation (3) takes on a negative sign for odd-numbered turnarounds, a positive sign for even-numbered turnarounds, and

$$\begin{cases} (x_2, y_2) = (x_1 \pm R, y_1 \mp R) \\ (x_3, y_3) = (x_1 \pm \partial w \mp R, y_1 - R) \\ (x_4, y_4) = (x_1 \pm \partial w, y_1) \end{cases}, \quad \begin{array}{l} \text{if } i \in \text{even\&} \ j \in \text{odd}, \partial = \frac{n_{unit}}{2} \\ \text{if } i \in \text{even\&} \ j \in \text{even}, \partial = \frac{n_{unit}}{2} - 1 \end{array}$$

i = 1,2...n, n is the number of planning units, and $n = round((n_{total} - 1)/(n_{unit} - 1))$; j = 1,2...$n_{unit}$.

By analogy, the turnaround function for counterclockwise operation can be inferred without further elaboration.

2.2.4. Fishtail-Turn Path Function

The fishtail-turn path is used to supplement the remaining operating rows after the planning unit and the turnaround of the horizontal operating area. For clockwise operation,

the schematic diagram of the vertical fishtail-turn path is illustrated in Figure 8a, and its turnaround path function is shown in Equation (4).

$$\begin{cases} y = \pm\sqrt{R^2 - (x - x_2)^2} + y_1, x_1 \le x < x_2 \\ y = y_2, x_3 \le x \le x_2 \\ y = \pm\sqrt{R^2 - (x - x_2)^2} + y_1, x_3 < x \le x_4 \end{cases} \tag{4}$$

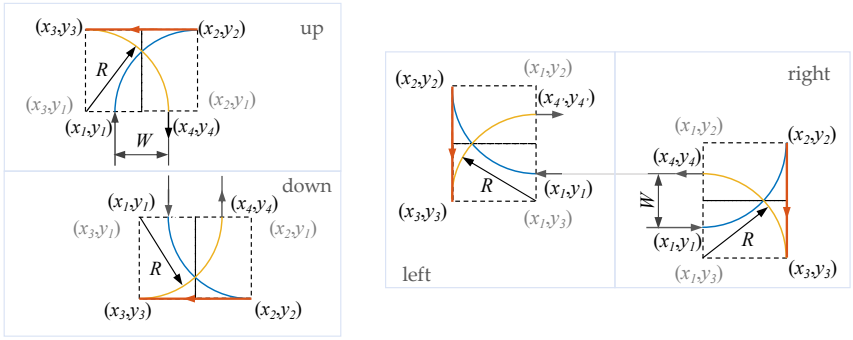

(**a**) (**b**)

Figure 8. Schematic diagram of the fishtail-turn path: (**a**) vertical; (**b**) horizontal.

Here, the upper fishtail function takes a positive sign, the lower one takes a negative sign, and $(x_2, y_2) = (x_1 + R, y_1 \pm R), (x_3, y_3) = (x_1 + w - R, y_1 \pm R), (x_4, y_4) = (x_1 + w, y_1)$.

The schematic diagram of the horizontal fishtail turnaround path is illustrated in Figure 8b, and its turnaround path function is shown in Equation (5).

$$\begin{cases} y = -\sqrt{R^2 - (x - x_1)^2} + y_2, x_1 \le x \le x_2, & \text{if } i \in \text{odd}, x_1 \le x < x_2 \\ & \text{if } i \in \text{even}, x_2 \le x < x_1 \\ y = y_2, x_3 \le x \le x_2 & \\ y = \sqrt{R^2 - (x - x_1)^2} + y_3, x_4 \le x \le x_3, & \text{if } i \in \text{odd}, x_4 \le x < x_3 \\ & \text{if } i \in \text{even}, x_3 \le x < x_4 \end{cases} \tag{5}$$

Here, $(x_2, y_2) = (x_1 \pm R, y_1 + R), (x_3, y_3) = (x_1 \pm R, y_1 + W - R), (x_4, y_4) = (x_1, y_1 + W)$, and the odd rows are taken as positive signs while even rows are negative; i = 1,2. . .n_y, n_y is the number of rows that require the fishtail turn.

2.3. Horizontal and Vertical Operation Connection Path

Contrary to the sequence of vertical and then horizontal operations during sowing, horizontal operations should be carried out first during harvesting to leave space for turnaround during vertical operations. Using the proper connection between horizontal and vertical operations is more conducive to reducing costs and improving the quality and efficiency of operations. The horizontal operation rows are generally 2 rows, and 4 rows after coordinate translation.

Considering the constraints of turning radius and turning area, the "Backward-Arc" (as shown in Figure 9a) and "Backward-Arc-Backward" (as shown in Figure 9b) methods are adopted to connect the horizontal and vertical operations so that the vehicle can return to the way that is favorable for vertical operation after the horizontal operation is completed, especially in terms of the heading, which should be in the same direction as the navigation line. "Backward" means reverse in a straight line. "Arc" refers to a quarter arc that is tangent to the reverse line and has a radius of R, and the function can be referred to the above bow-turn function, or the parametric equations of the circle, as shown in Equation (6). An example of the horizontal and vertical connections are displayed in Figure 9c, where the length of the vertical operation has been reduced to emphasize the connection. The "Backward" before the "Arc" (shown by the blue dotted line in Figure 9) is a non-essential

option, depending on the specifics of the job, and is not selected if the least amount of backward movement is the priority or is selected if the operation coverage is the priority.

$$\begin{cases} x = R\cos\theta + a \\ y = R\sin\theta + b \end{cases}, 0 \le \theta \le 2\pi \quad (6)$$

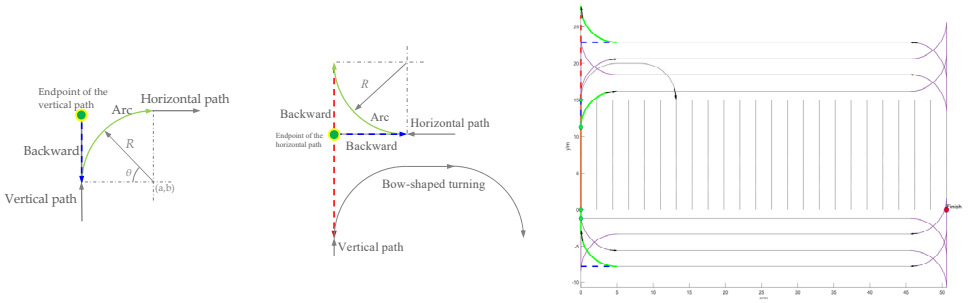

(**a**) (**b**) (**c**)

Figure 9. Schematic diagram of the horizontal and vertical operation connection path. (**a**) Backward–Arc; (**b**) Backward–Arc–Backward; (**c**) application examples.

Here, (a, b) are the coordinates of the circle center and θ is the angle of the circle center.

2.4. Obstacle Avoidance Path

Obstacle avoidance paths can be viewed as local path planning based on global paths and maps. There is no direct obstacle contour size in the sowing navigation data. When there is a certain distance break in the navigation data within the operating row and there is a detour trajectory (e.g., at a in Figure 1), it is determined that an obstacle has been encountered.

2.4.1. Obstacle Avoidance Strategy

Obstacle avoidance paths are generated based on the determination of the turnaround path and operation routing.

(1) When the obstacle is at or near the end of the operation line, and there is not enough space for obstacle avoidance in the adjacent safety row, it can choose to turn in advance for obstacle avoidance, such as at IV in Figure 10. It may adopt the way backward– bow turn–backward to avoid obstacles, that is, reverse the distance *R* at the obstacle endpoint, start the bow turn to the corresponding operation line, and then reverse to the beginning of that line. Bow turn is a necessary option, and the two "backward" parts are optional, depending on the actual need of the operation coverage.

(2) When obstacles are not at the end of the operation line, since the specific sizes and shapes of the obstacles are unknown, while the path with navigation data is assumed to be a safe path, the obstacle avoidance is prioritized along the nearest safe operating line, followed by the choice of the region where the operation has been completed, and the order can be adjusted depending on the actual situation. Given the unknown shapes, sizes, and locations of obstacles, the start point of avoidance is moved *R* from the breakpoints to both ends to ensure safety. The moving path can also be realized by reverse operation so that the operation line is without omission.

For example, a small amount of vehicle traffic in the unharvested area has little impact on the recycling effect when recycling residual film. Moreover, due to the sowing width being larger than the residual film recycling width, data loss within a single sowing row will result in missing data in adjacent rows within the same segment after coordinate translation, as shown in Figure 10, I and III. Cotton harvesting when the vehicle is not recommended to pass through the unharvested area; it is prioritized to select the completed harvesting area, as shown in Figure 10, I and II.

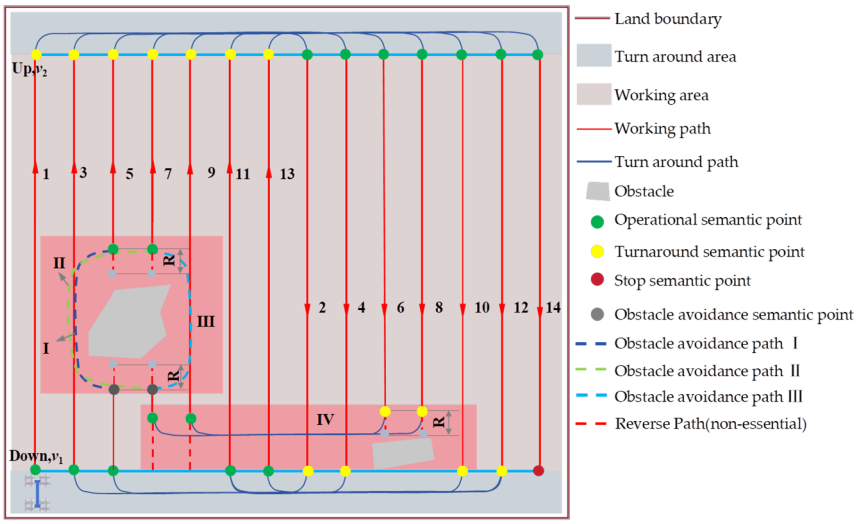

Figure 10. Schematic diagram of obstacle avoidance path.

2.4.2. Obstacle Avoidance Path Generation Methods

Maximum curvature constraint needs to be considered for curve fitting instead of being directly based on the known points since obstacle avoidance is limited by the minimum turning radius. Two ways of obstacle avoidance path generation (when the obstacle is not at the end) are proposed below.

(1) Generation by circular arcs and straight lines

The obstacle avoidance path depends on the obstacle avoidance width nW and the obstacle length L. There are mainly four ways. ① When $nW \leq R$ and $L \leq 2R$, the obstacle avoidance path is arc–semicircle–arc, as displayed in Figure 11a. ② When $nW \leq R$ and $L \geq 2R$, the path is arc–arc–line–arc–arc, as displayed in Figure 11b. ③ When $nW \geq R$ and $L < 2R$, the path is arc–line– semicircle–line–arc, as displayed in Figure 11c. ④ When $nW > R$ and $L > 2R$, the path is arc–line–arc–line–arc–line–arc, as displayed in Figure 11d. The distance calculation of the obstacle avoidance path for the four ways is in Equation (7).

$$\begin{cases} D = 2\pi R, nW \leq R \& L \leq 2R \\ D = 2\pi R + L - 2R = 2R(\pi - 1), nW \leq R \& L \geq 2R \\ D = 2\pi R + nW - R = R(2\pi - 1) + nW, nW > R \& L < 2R \\ D = 2\pi R + nW - R + L - 2R = R(2\pi - 3) + nW + L, nW > R \& L > 2R \end{cases} \tag{7}$$

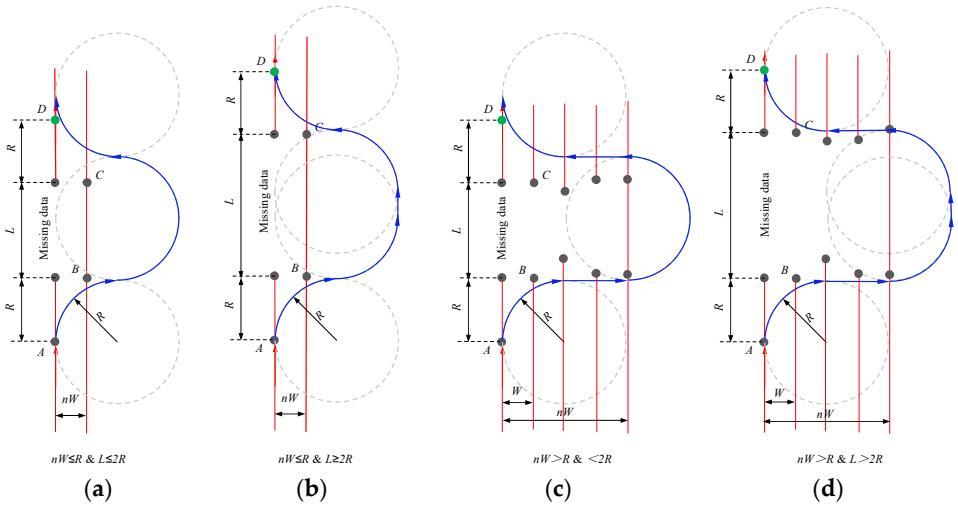

Figure 11. Schematic diagram of circular arc–linear obstacle avoidance path. (**a**) Arc–semicircle–arc; (**b**) arc–arc–line–arc–arc; (**c**) arc–line–semicircle–line–arc; (**d**) arc–line–arc–line–arc–line–arc.

It can be seen that the circular arc–linear path function acquisition is simple and easy to implement; however, it is not optimal in terms of obstacle avoidance distance.

(2) Generation by cubic spline interpolation

The cubic spline curve has good smoothness, avoiding corners and abrupt changes. The curve shape can be controlled by adjusting the position of control points and is simple and efficient to calculate [29,30]. Therefore, the cubic spline interpolation method is used to generate the obstacle avoidance path in this paper.

The obstacle avoidance problem can be simply described as solving a cubic spline curve with four known points A, B, C, and D, as shown in Figure 12. However, different from the ordinary cubic spline interpolation method that directly fits the curve based on known points, subject to the influence of the turning radius, it is necessary to add the constraints that the maximum curvature of the path $\leq 1/R$ and the tangent lines of starting and ending points A and D are the same as the operation row. The operation cost is also considered, i.e., the operation path is expected to be the shortest. Therefore, the obstacle avoidance path generation can be converted into an optimization problem with minimum distance interpolation conditions and maximum curvature constraints, i.e., finding the spline curve through the four points A, B, C, and D with the shortest distance while satisfying the curvature requirement.

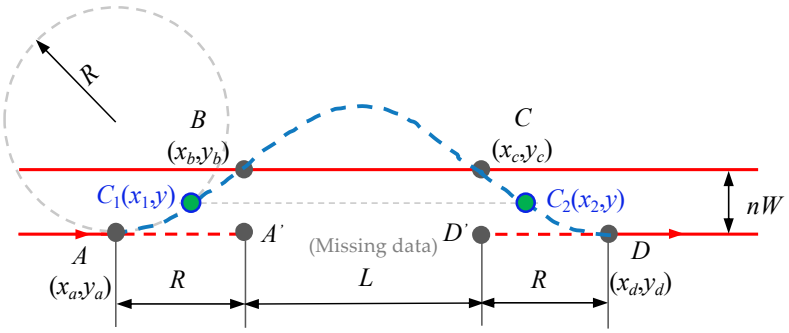

Figure 12. Schematic diagram of obstacle avoidance requirements.

A curve that is graceful and not usable may be generated (as shown in Figure 13) if the obstacle avoidance path is solved based only on the known four points without considering the curvature constraints. It is considered prudent to add symmetric control points C_1 (x_1, y) and C_2 (x_2, y) to solve this problem according to the principle of optimization and curve generation; then, the solution equation of cubic spline curve is as follows:

$$\begin{cases} x = [x_a, x_b, x_c, x_d] \\ y = [y_a, y_b, y_c, y_d] \\ S(x_a)' = 0 \\ S(x_d)' = 0 \\ S = spline(x, [0, y, 0]) \end{cases} \Rightarrow \begin{cases} x = [x_a, x_1, x_b, x_c, x_2, x_d] \\ y = [y_a, y, y_b, y, y_d] \\ S(x_a)' = 0 \\ S(x_d)' = 0 \\ S = spline(x, [0, y, 0]) \end{cases} \quad (8)$$

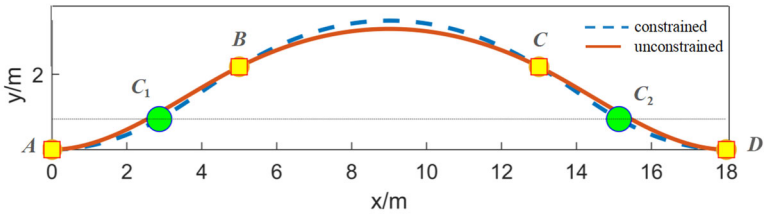

Figure 13. Example of avoidance path generation.

Here, S represents the cubic spline curve; *spline* represents the function to solve the spline curve.

The control points are a set. To find the optimal control points while considering the cost of obstacle avoidance, the objective is converted to solve for the path with the shortest obstacle avoidance distance under the maximum curvature constraint. The objective function can be described as follows:

$$\min_{x_x=[x_1,x_2,y]}(D_S)\begin{cases} k_{\max}-1/R\le 0 \\ lb\le x_x\le ub \\ lb=[x_a,x_c,y_a] \\ ub=[x_b,x_d,y_b] \end{cases} \tag{9}$$

Here, D_S is the distance of the obstacle avoidance path; x_x is the coordinates of the control point; k_{max} is the maximum curvature of the curve, $k_{\max}=\max[|S''(x_D)|]$; lb and ub are the lower and upper limits of the control point, respectively.

The equation for solving D_s is as follows:

$$\begin{cases} x_D=linspace[x_{start},max(x),n_x] \\ y_D=ppval(\mathrm{S},x_D) \\ D_S=sum\{hypot[diff(x_D),diff(y_D)]\ \} \end{cases} \tag{10}$$

Here, *linspace* denotes the generation of a linear spacing vector function; x_D denotes an equally spaced vector from x_{start} to the maximum x-coordinate value, containing n_x points for discrete sampling on a spline interpolation curve; *ppval* denotes the function to compute a piece-wise polynomial; y_D denotes the y-coordinate value obtained by interpolating the points on the vector x_D using the spline interpolation curve S; *diff* denotes the function that computes the difference between two adjacent elements, i.e.,

$$\begin{aligned} diff(x_D)&=[x_D(2)-x_D(1)\ ,x_D(3)-x_D(2)\ ,\dots\ ,x_D(n_x)-x_D(n_x-1)] \\ diff(y_D)&=[y_D(2)-y_D(1)\ ,y_D(3)-y_D(2),\ \dots\ ,y_D(n_x)-y_D(n_x-1)] \end{aligned}$$

hypot denotes the Euclidean norm at the corresponding position of the input vector, i.e., the square root of the sum of squares; *sum* denotes the summation function.

Take A (0,0), B (5,2.2), C (13,2.2), and D (18,0) as an example to solve the shortest obstacle avoidance path when the minimum turning radius is 5 m, as shown in Figure 13, where the coordinates of the control point C_1 is (2.8675,0.8109), C_2 is (15.1325,0.8109), the shortest curve length D_S = 19.5937, and the minimum value of k_{max} is 0.1972. The vehicle is able to turn and the obstacle avoidance path distance is significantly smaller than that of the circular arc–linear mode. In the unconstrained condition i.e., solving the obstacle avoidance curve only by four points A, B, C, and D, the shape is similar to the constrained solving result, yet its maximum curvature is 0.3269, which cannot satisfy the vehicle turning demand.

In summary, both the circular arc–linear method and the constrained cubic spline interpolation method can accomplish the obstacle avoidance tasks, but it is evident that the latter has a lower one in terms of operation cost. This paper gives priority to the cubic spline interpolation method.

2.5. Operation Semantics

Different from intelligent driving cars, in intelligent agricultural machinery, it is more important to complete the relevant operations besides walking, which involve lifting and lowering of implements, changing speeds, etc., i.e., completing the relevant operations according to the instructions at the specified path points. Therefore, semantics are embedded in the prior paths so that the machine in question gets explicit and specific instructions at the designated point, thus better coordinating the relationship between walking and operation and realizing the orderly control of vehicle auto-driving operation.

There are four main semantic points included in the working process, as depicted in Figure 14. The whole working process contains operation, turnaround, and stop semantic points at least, and the obstacle avoidance semantic points depend on whether there

are obstacles in the working scene or not. Semantic embedding is carried out based on the determination of the turnaround path, operation route, and obstacle avoidance path and flag bits are configured for them. When the vehicle position coordinates match the operational semantic points during control, the corresponding command is triggered to execute the corresponding action.

Number	Type	Functional instructions
1	Operational semantic point	Device down, operating speed v_1
2	Turnaround semantic point	Device up, turnaround speedv_2
3	Obstacle avoidance semantic point	Device up, obstacle avoidance speed v_2
4	Stop semantic point	Device up, vehicle stop

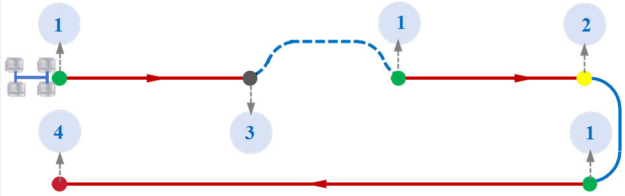

Figure 14. Schematic diagram of embedding semantics.

2.6. Path Generation Software

The path generation software has been designed based on MATLAB APP (2021b), and the operation interface is demonstrated in Figure 15. By importing the processed navigation sowing data or manually inputting the data, new paths suitable for auto-driving operation can be generated according to the operation direction, turning radius, operation width, etc. The newly generated paths can be saved as CSV or TXT documents, numbered, and stored in the prior map library so that the relevant maps can be called up for operation during the subsequent path tracking control.

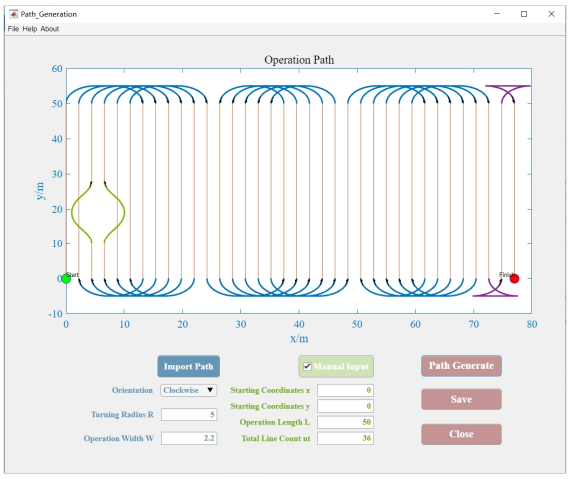

Figure 15. Path generation software interface (Version 1.0).

3. Results and Discussion

3.1. Simulation Test

The operation path is generated by simulating the given parameters, such as the operation direction (clockwise or counterclockwise), starting point coordinates, operation row length, total number of operation rows, turning radius, and operation width, based on the above path generation software.

Without considering the horizontal operations, the operation width is set to 2.2 m, the turning radius is 5 m, the total number of operation rows is 42, and the obstacle information is given. Then the optimal n_{uint} is calculated to be 14, the number of planning units n is 3,

the number of remaining rows is 2, and the maximum curvature of the obstacle avoidance path is 0.1972, which meets the curvature constraints. The planning unit adopts the bow turn, and the remaining rows adopt the fishtail turn, which can connect all the operation rows, and the full coverage of the operation path can be achieved by considering reversing when avoiding obstacles. The generated path is shown in Figure 16.

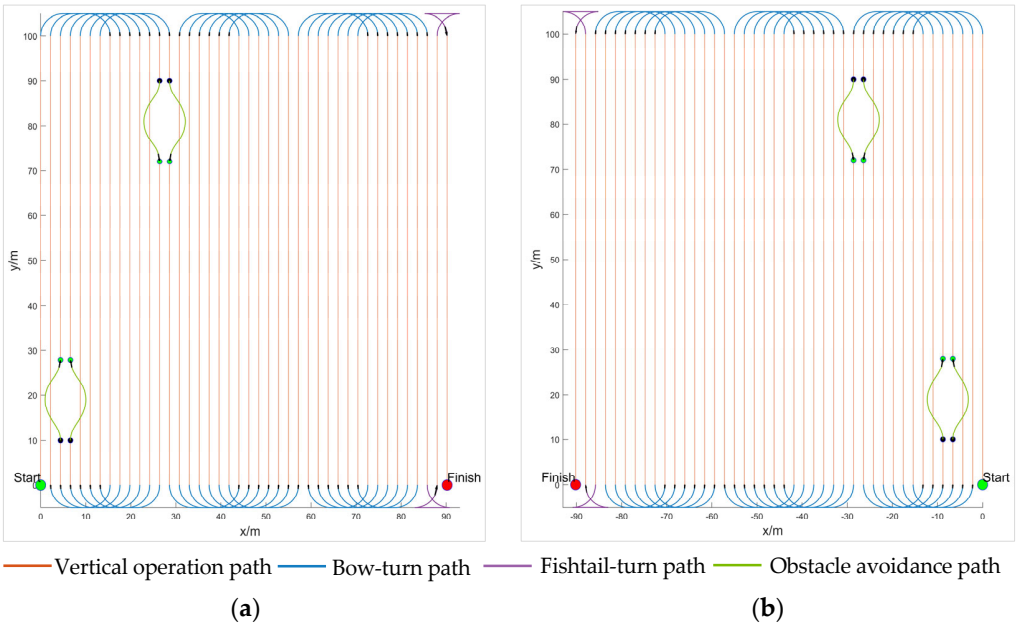

Figure 16. Examples of simulation paths without considering lateral operations. (**a**) Clockwise operation; (**b**) counterclockwise operation. Note: The blank area in the operation line indicates the obstacle area (the same as below).

Considering the horizontal operations, the operation width is set to 2.2 m, the turning radius is 5 m, and the total number of operation rows is 25. Then, the optimal n_{uint} is calculated to be 12, n is 2, and the number of remaining rows is 2. The simulation results are presented in Figure 17, where the length of the vertical operation rows has been reduced to emphasize the horizontal operations. When there are sufficient turnaround spaces at both horizontal ends, there are 3R operation lengths missing (shown by the red dashed line in Figure 17), and of course, these sections can be fully covered by reversing, as shown in Figure 17a. When considering the turnaround area constraint, i.e., it is unknown whether there is enough turnaround space or is known to be small, there are 15R operational lengths missing, and similarly, these parts can be realized by reversing to achieve full coverage, as shown in Figure 17b. Whether to reverse or not depends on the actual operation requirements and the turning characteristics of the vehicle, i.e., whether to emphasize operational efficiency or operational coverage. The simulation parameters are changed to real values that can obtain the actual operation path.

The first step is to perform horizontal operations in the direction of the starting point during path tracking. Then, the vertical operation row nearest to the starting point, i.e., the first row of the vertical area, is connected by the horizontal–vertical connection method of "Backward-Arc" to go to the horizontal operation area in the opposite direction. Finally, it returns to the end of the first row of the vertical area by the connection method of "Backward-Arc-Back" and starts the bow nesting operations and the fishtail supplementary turnarounds in the vertical area until the end of the operation.

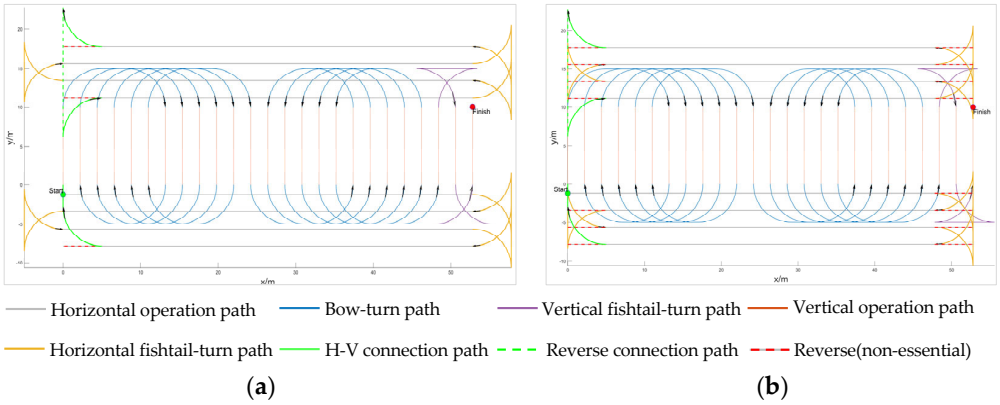

Figure 17. Simulation path considering the lateral operation: (**a**) when there is sufficient horizontal turnaround area; (**b**) considering horizontal turnaround area constraints.

3.2. Field Test

Based on the sowing navigation data of a certain planter (one machine with two films) in Bazhou, Xinjiang on 16–18 April 2024, the basic path data were obtained after function point marking, coordinate translation, coordinate transformation, etc. Considering the privacy of the operating plots, the coordinate values shown in the following figures are in error compared to the actual values while the length of the vertical operation has been reduced for the convenience of display. Cotton planted with plastic film needs to be recycled after harvesting, with a self-propelled residual film recycling machine as the object machine; the operation width is 2.2 m and the turning radius is set to 5 m.

Operational effectiveness is evaluated in terms of the operation coverage ratio C_R and the operation distance ratio D_R. Different from the way of calculating the operation coverage ratio of sowing, C_R is related to the total length of actual operation L_{wt} and the total length of sowing L_{st}. D_R is related to the operation distance D_w ($D_{w=}$ L_{wt}) and the total traveled distance D_t. The larger the operation coverage ratio and distance ratio is, the better the operation effect will be.

$$C_R = \frac{L_{wt}}{L_{st}} \times 100\% \tag{11}$$

$$D_R = \frac{D_w}{D_t} \times 100\% \tag{12}$$

For the relatively regular plot, the operational plot on April 18 was used as the study object, recorded as plot A. The original map of the plot refers to Figure 1. The new path after adding the turnaround, obstacle avoidance, and horizontal and vertical connection paths is shown in Figure 18.

Except for the necessary reversing paths during the fishtail turn and horizontal–vertical connections, the operation coverage ratio C_R was 98.6%, and the distance ratio D_R was 87.93% when the non-necessary reversing operations and obstacles were not taken into account, as shown in Table 1. C_R rose as the plot area grew since operational omission mainly occurs during horizontal turning, horizontal and vertical connection, and obstacle avoidance and does not change as the plot area changes. When considering obstacles, both C_R and D_R decreased accordingly depending on the number of obstacles, with each additional obstacle increasing the 4R missed. Of course, as the analysis in Section 2 has shown, if non-necessary reversing is considered, the full coverage of the operating row can be achieved, but D_R will be reduced accordingly.

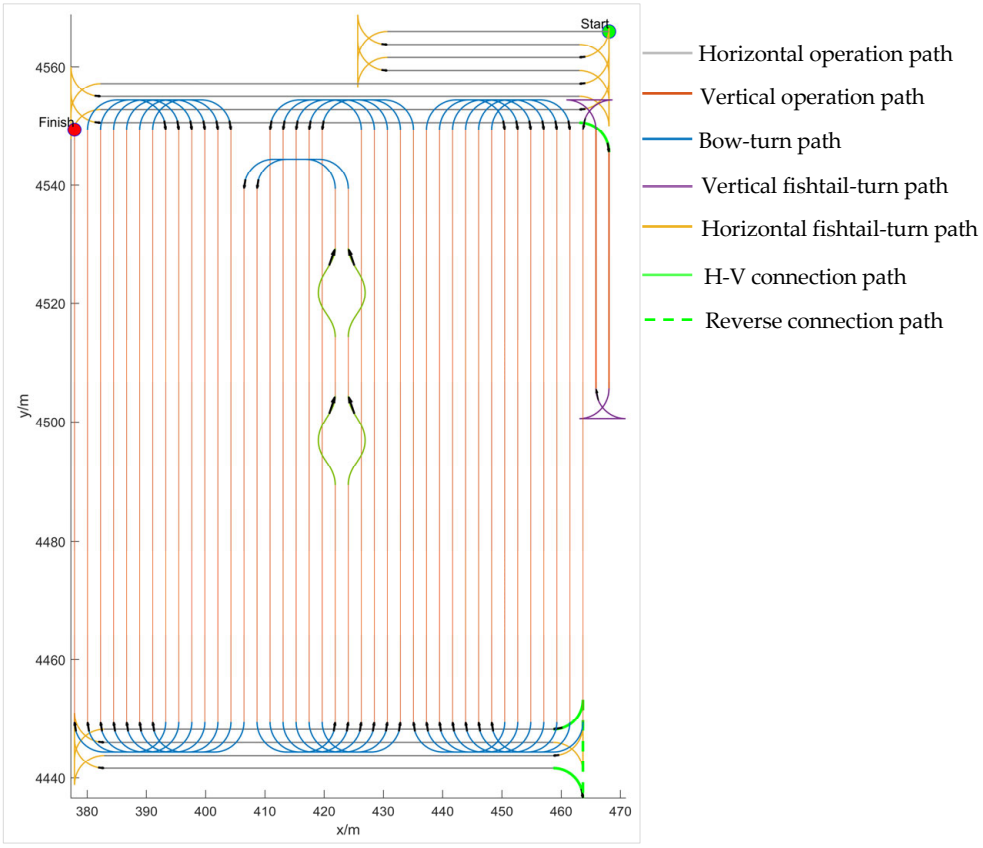

Figure 18. Planning path of plot A.

Table 1. Evaluation indicators for path planning of plot A.

Evaluation Indicators		Disregard Non-Essential Reversing	Considering Non-Essential Reversing
Not considering obstacles	Operation coverage ratio C_R/%	98.60	100
	Operation distance ratio D_R/%	87.93	86.52
Considering obstacles	Operation coverage ratio C_R/%	97.93	100
	Operation distance ratio D_R/%	87.49	85.41

We took operation plots on April 16 and 17 as the study objects, as shown in Figure 19a. As the same plot finished the sowing operation in two days, the plots on the 16th and 17th were combined and recorded as plots B_1 (left side in Figure 19b) and B_2 (right side in Figure 19b), respectively. For relatively irregular plots, path planning is carried out according to the above method after dividing them into sub-plots, and when the calculated number of planning units $n < 2$, the plot is operated as a whole, i.e., the overall unit method is used to minimize the number of reversals. The path planning evaluation indicators for plots B_1 and B_2 are shown in Table 2. When non-essential reversing and obstacles are not considered, C_R values were 98.21% and 98.46%, and D_R values were 86.89% and 89.64%, respectively. There was a corresponding decrease when obstacles were considered, with C_R values of 97.93% and 97.61% and D_R values of 85.13% and 88.52%. Similar to plot A, the full coverage of the operational rows could be achieved with reversing, but there was a corresponding reduction in D_R.

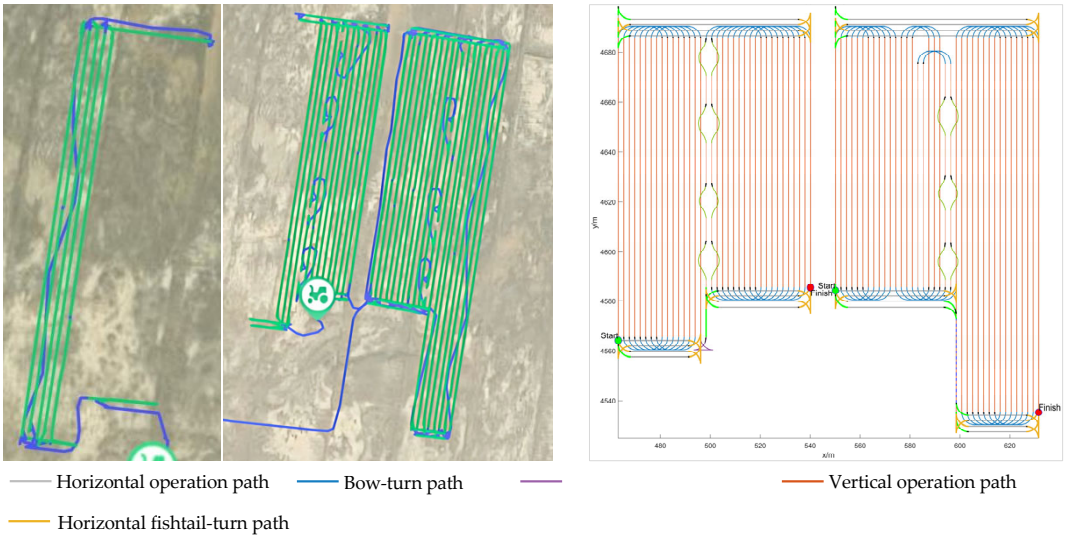

Figure 19. Planning paths of plots B_1 and B_2: (**a**) navigation paths; (**b**) planned path.

Table 2. Evaluation indicators for path planning of plots B_1 and B_2.

Evaluation Indicators		Plot B_1		Plot B_2	
		Disregard Non-Essential Reversing	**Considering Non-Essential Reversing**	**Disregard Non-Essential Reversing**	**Considering Non-Essential Reversing**
Not considering obstacles	Operation coverage ratio C_R/%	98.21	100	98.46	100
	Operation distance ratio D_R/%	86.89	85.10	89.64	88.10
Considering obstacles	Operation coverage ratio C_R/%	97.23	100	97.61	100
	Operation distance ratio D_R/%	85.13	82.43	88.52	86.13

3.3. Discussion

Sowing rows limits the operating range of subsequent plant protection, harvesting, and residual film recycling. It is more conducive to planning practical operation paths, improving planning accuracy, and reducing planning costs when path planning for subsequent operations is based on sowing navigation data. The goal of path planning is mainly to be able to cover all the operating rows and minimize the cost at this time, but it is also constrained by factors such as the vehicle turning radius and turning area.

Under the constraints, the bow turn and fishtail turn have smaller requirements on the turnaround width compared to the Ω turn, making them suitable for practical applications with larger turning radii; the turnaround strategy of dividing the planning unit has a smaller distance cost, the obstacle avoidance path of the cubic spline curve can effectively generate the obstacle avoidance path, and the "Backward-Arc" and " Backward-Arc-Backward" methods can realize the connection of horizontal and vertical operations. The feasibility of the above methods was verified by both simulation and field tests. Local connections and detours are usually challenging for path planning, and local path planning like horizontal operations and obstacle avoidance are the main factors generating performance differences, but with increasing plot sizes, the smaller the proportion of local path planning to the overall planning is, the better the operational performance will be. Operation omission mainly occurs in horizontal operation, horizontal–vertical connection, and obstacle avoidance paths, and the test results reveal that without considering horizontal operation and obstacle avoidance, the vertical area can realize the full coverage of operation rows. When the horizontal operation is considered, the full coverage of the working rows can be achieved with the use of the non-essential reversing operation, and even if the reversing operation is not considered and obstacles are taken into account, C_R can reach more than 97%. This

value is positively correlated with the operational area of the plot, and the larger the plot is, the more obvious the advantages of the method proposed in the article will be.

Most of the plots were relatively regular in shape, but for a few heterogeneous plots, the adaptability of the proposed method was inferior and needed to be combined with cluster intelligence algorithms to improve the adaptability of the method in subsequent research. The proposed method is based on sowing navigation data. If these data are significantly erroneous or even lost due to hardware failures, improper operations, harsh operating conditions, or other factors, it will directly affect the planning effectiveness, and date loss will invalidate the method even more. Moreover, there is still a certain threshold to obtain sowing navigation data for cotton or other crops currently, which is mainly concentrated in the enterprises of assisted driving products. It is of great value and significance to accelerate the comprehensive openness and integration of prior information and realize the sharing and interoperability of agricultural big data.

4. Conclusions

On the basis of coordinate marking, coordinate translation, and the transformation of obstacle breakpoints and endpoints of operation rows for sowing navigation data, path planning was carried out according to the generation methods of paths for turnaround, obstacle avoidance, and horizontal and vertical operation connection combined with vehicle turning radius and planting agronomic constraints. The main conclusions are as follows:

- The characteristics of typical turnaround methods were analyzed and the bow turn was preferred due to the advantages of a smaller turnaround area and no need for reversing. The turnaround strategies for the overall operation and the dividing planning units were proposed and prioritized to the latter considering the distance cost, and the path cost function was given to determine the optimal n_{uint} and n. Considering the situation that $(n_{total} - 1)/(n_{unit} - 1)$ cannot be divisible, and horizontal operation, the fishtail turn was used as a supplement, and the path functions of bow turn and fishtail turn were given. The connection methods of "Backward-Arc" and " Backward-Arc-Backward" were proposed to realize the smooth connection of horizontal and vertical operations. The operation routing could be determined based on the above path determination.
- Obstacle avoidance paths of circular arc–linear and cubic spline curves were proposed, and the latter was preferred given the distance cost. Different from the ordinary cubic spline curve generation, the obstacle avoidance path is subject to the minimum turning radius constraint and the objective claim of the shortest distance, so the obstacle avoidance path generation was converted into solving an optimization problem with interpolation conditions and maximum curvature constraints and the objective function was given. Considering the dual attributes of walking and the operation of agricultural machinery, four kinds of semantic points, namely operation, turnaround, obstacle avoidance, and stopping, were embedded in the path, and the corresponding functional commands were clarified.
- The MATLAB-APP-based path generation software was validated through simulation and field tests, showing $C_R \geq 98.21\%$ and $D_R \geq 86.89\%$ disregarding non-essential reversing and obstacles, and C_R increased with the plot area. Both C_R and D_R declined when obstacles were considered, and the more obstacles there were, the faster the decrease was, with $C_R \geq 97.23\%$ and $D_R \geq 85.13\%$. Considering non-essential reversing ensured the full coverage of the operating rows but slightly reduced D_R, with $D_R \geq 85.10\%$ without obstacles and $D_R \geq 82.43\%$ when considering obstacles.

In summary, path planning based on the prior sowing paths is feasible and favorable for obtaining practical target paths, improving the accuracy of path planning, and reducing the planning cost and is well adapted to the scenarios of existing crop coverage and requires precise row alignment. This method has some reference value for path planning for other field crops such as corn and processing tomato. Compared to the operating environments of road vehicles, the farmland environment is relatively closed. Integrating

land boundary detection, obstacle calibration, and in-field path planning to form high-precision maps with prior information that are more suitable for the automated driving of agricultural machinery, and establishing an operational map library, is one of the focuses of future research.

Author Contributions: Conceptualization, M.W. and X.T.; writing—original draft preparation, M.W. and X.T.; software, M.W., C.N. and Z.W.; validation, M.W. and C.N.; writing—review and editing, C.N., Z.W., Y.J. and J.J. All authors have read and agreed to the published version of the manuscript.

Funding: This research was funded by the Key Research and Development Program Project of the Xinjiang Uygur Autonomous Region (2022B02022-4) and the Central Guidance Local Science and Technology Development Special Fund Project (ZYYD2023C08).

Institutional Review Board Statement: Not applicable.

Data Availability Statement: The data presented in this study are available on request from the corresponding author.

Conflicts of Interest: The authors declare no conflicts of interest.

References

1. Zhao, Y.; Chen, X. Problems and Prospects of High Quality Cotton Production in China. *J. Tarim Univ.* **2023**, *35*, 1–8.
2. National Statistics Office Announcement on Cotton Production in 2023. Available online: https://www.stats.gov.cn/xxgk/sjfb/zxfb2020/202312/t20231225_1945749.html (accessed on 17 June 2024).
3. Bochtis, D.D.; Vougioukas, S.G. Minimising the Non-Working Distance Travelled by Machines Operating in a Headland Field Pattern. *Biosyst. Eng.* **2008**, *101*, 1–12. [CrossRef]
4. Yang, T.; Jin, C.; Ni, Y.; Liu, Z.; Chen, M. Path Planning and Control System Design of an Unmanned Weeding Robot. *Agriculture* **2023**, *13*, 2001. [CrossRef]
5. Meng, Z.; Liu, H.; Wang, H.; Fu, W. Optimal path planning for agricultural machinery. *Trans. Chin. Soc. Agric. Mach.* **2012**, *43*, 147–152.
6. Zhou, J.; He, Y. Research Progress on Navigation Path Planning of Agricultural Machinery. *Trans. Chin. Soc. Agric. Mach.* **2021**, *52*, 1–14.
7. Meng, Z.; Wang, H.; Fu, W.; Liu, M.; Yin, Y.; Zhao, C. Research Status and Prospects of Agricultural Machinery Autonomous Driving. *Trans. Chin. Soc. Agric. Mach.* **2023**, *54*, 1–24.
8. Liu, C.; Zhao, X.; Du, Y.; Cao, C.; Zhu, Z.; Mao, E. Research on Static Path Planning Method of Small Obstacles for Automatic Navigation of Agricultural Machinery. *IFAC-PapersOnLine* **2018**, *51*, 673–677. [CrossRef]
9. Xi, X.; Shi, Y.; Shan, X.; Zhang, Q.; Jin, Y.; Gong, J.; Zhang, J.; Zhang, R. Obstacle Avoidance Path Control Method for Agricultural Machinery Automatic Driving Based on Optimized Bezier. *Trans. Chin. Soc. Agric. Eng.* **2019**, *35*, 82–88.
10. Cariou, C.; Gobor, Z.; Seiferth, B.; Berducat, M. Mobile Robot Trajectory Planning Under Kinematic and Dynamic Constraints for Partial and Full Field Coverage. *J. Field Robot.* **2017**, *34*, 1297–1312. [CrossRef]
11. Boryga, M.; Kołodziej, P.; Gołacki, K. Application of Polynomial Transition Curves for Trajectory Planning on the Headlands. *Agriculture* **2020**, *10*, 144. [CrossRef]
12. Zhang, C.; Lu, B.; Li, Q.; Wang, D.; Xiong, Z.; Ding, Y. Unmanned Seeding Automatic Control Method of Rapeseed Based on Two-back and Three-cut Fishtail U-turn Model. *Trans. Chin. Soc. Agric. Mach.* **2022**, *53*, 66–75.
13. Boryga, M. Trajectory Planning for Tractor Turning Using the Trigonometric Transition Curve. *Agric. Eng.* **2023**, *27*, 203–212. [CrossRef]
14. Hu, X.; Chen, L.; Tang, B.; Cao, D.; He, H. Dynamic Path Planning for Autonomous Driving on Various Roads with Avoidance of Static and Moving Obstacles. *Mech. Syst. Signal Process.* **2018**, *100*, 482–500. [CrossRef]
15. Zhao, X.; Wang, K.; Wu, S.; Wen, L.; Chen, Z.; Dong, L.; Sun, M.; Wu, C. An Obstacle Avoidance Path Planner for an Autonomous Tractor Using the Minimum Snap Algorithm. *Comput. Electron. Agric.* **2023**, *207*, 107738. [CrossRef]
16. Xu, L.; You, J.; Yuan, H. Real-Time Parametric Path Planning Algorithm for Agricultural Machinery Kinematics Model Based on Particle Swarm Optimization. *Agriculture* **2023**, *13*, 1960. [CrossRef]
17. Wu, X.; Bai, J.; Hao, F.; Cheng, G.; Tang, Y.; Li, X. Field Complete Coverage Path Planning Based on Improved Genetic Algorithm for Transplanting Robot. *Machines* **2023**, *11*, 659. [CrossRef]
18. Höffmann, M.; Patel, S.; Büskens, C. Optimal Coverage Path Planning for Agricultural Vehicles with Curvature Constraints. *Agriculture* **2023**, *13*, 2112. [CrossRef]
19. Wu, X.; Bai, J.; Li, X.; Hao, F. Smooth Path Planning Method of Agricultural Vehicles Based on Improved Hybrid A*. In Proceedings of the 2023 IEEE 3rd International Conference on Information Technology, Big Data and Artificial Intelligence (ICIBA), Chongqing, China, 26–28 May 2023; pp. 664–668.

20. Šelek, A.; Seder, M.; Brezak, M.; Petrović, I. Smooth Complete Coverage Trajectory Planning Algorithm for a Nonholonomic Robot. *Sensors* **2022**, *22*, 9269. [CrossRef]
21. Oksanen, T.; Visala, A. Coverage Path Planning Algorithms for Agricultural Field Machines. *J. Field Robot.* **2009**, *26*, 651–668. [CrossRef]
22. Höffmann, M.; Patel, S.; Büskens, C. Optimal Guidance Track Generation for Precision Agriculture: A Review of Coverage Path Planning Techniques. *J. Field Robot.* **2024**, *41*, 823–844. [CrossRef]
23. Chen, K.; Xie, Y.; Li, Y.; Liu, C.; Mo, J. Full Coverage Path Planning Method of Agricultural Machinery under Multiple Constraints. *Trans. Chin. Soc. Agric. Mach.* **2022**, *53*, 17–26+43.
24. Zhai, W.; Wang, D.; Chen, Z.; Dong, L.; Zhao, X.; Wu, C. Autonomous Operation Path Planning Method for Unmanned Agricultural Machinery. *Trans. Chin. Soc. Agric. Eng.* **2021**, *37*, 1–7.
25. Mechanization Rate Reaches 100%! Xinjiang Cotton Planting with Beidou. Available online: http://www.beidou.gov.cn/yw/xwzx/202404/t20240430_27890.html (accessed on 17 August 2024).
26. Zhou, H. Study on the Evolution of Cotton Cultivation Technology in Xinjiang Production and Construction Corps. Master's Thesis, Huazhong University of Science and Technology, Wuhan, China, 2024.
27. Ny, J.; Feron, E.; Frazzoli, E. On the Dubins Traveling Salesman Problem. *IEEE Trans. Autom. Control* **2012**, *57*, 265–270.
28. Manyam, S.; Rathinam, S. On Tightly Bounding the Dubins Traveling Salesman's Optimum. *J. Dyn. Syst. Meas. Control* **2018**, *140*, 071013. [CrossRef]
29. Li, W.; Tan, M.; Wang, L.; Wang, Q. A Cubic Spline Method Combing Improved Particle Swarm Optimization for Robot Path Planning in Dynamic Uncertain Environment. *Int. J. Adv. Robot. Syst.* **2020**, *16*, 172988141989166. [CrossRef]
30. Ma, X.; Gong, R.; Tan, Y.; Mei, H.; Li, C. Path Planning of Mobile Robot Based on Improved PRM Based on Cubic Spline. *Wirel. Commun. Mob. Comput.* **2022**, *2022*, 1632698. [CrossRef]